Article

Cell Reports

Acute *Plasmodium* Infection Promotes Interferon-Gamma-Dependent Resistance to Ebola Virus Infection

Graphical Abstract

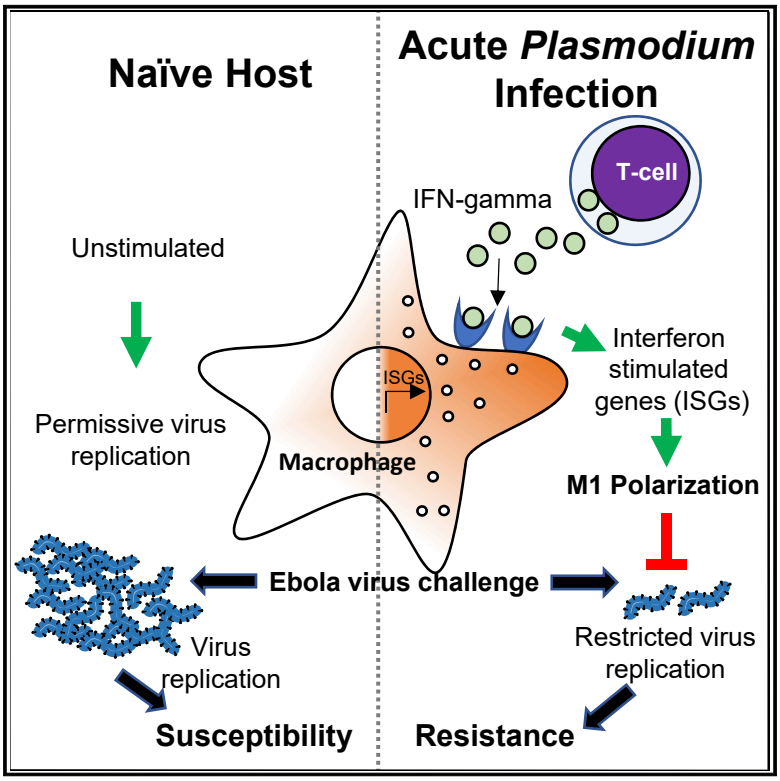

Authors

Kai J. Rogers, Olena Shtanko, Rahul Vijay, ..., Mary R. Galinski, Noah S. Butler, Wendy Maury

Correspondence

wendy-maury@uiowa.edu

In Brief

Rogers et al. demonstrate that acute *Plasmodium* infection protects against lethal Ebola virus challenge. Protection is conferred by *Plasmodium*-elicited interferon gamma (IFN-γ) that causes M1 polarization of tissue macrophages. These studies provide insight into conflicting clinical data regarding whether malaria protects or sensitizes hosts to Ebola virus.

Highlights

- Acute *Plasmodium* infection protects mice against lethal Ebola virus challenge
- Protection is conferred by *Plasmodium*-elicited IFN-γ polarization of tissue macrophages
- Protection is transient, and supraphysiological EBOV doses abrogate animal protection
- Some *Plasmodium*-protected mice elicit a robust antibody response against the virus

Rogers et al., 2020, Cell Reports *30*, 4041–4051
March 24, 2020
https://doi.org/10.1016/j.celrep.2020.02.104

CellPress

Cell Reports
Article

Acute *Plasmodium* Infection Promotes Interferon-Gamma-Dependent Resistance to Ebola Virus Infection

Kai J. Rogers,[1] Olena Shtanko,[2] Rahul Vijay,[1] Laura N. Mallinger,[1] Chester J. Joyner,[3,4] Mary R. Galinski,[4,5] Noah S. Butler,[1,6] and Wendy Maury[1,6,7,*]

[1]Department of Microbiology and Immunology, University of Iowa, Iowa City, IA 52242, USA
[2]Host-Pathogen Interactions, Texas Biomedical Research Institute, San Antonio, TX 78227, USA
[3]Division of Pulmonary, Allergy, Critical Care & Sleep Medicine, Department of Medicine, Emory University, Atlanta, GA 30322, USA
[4]Malaria Host-Pathogen Interaction Center, Emory Vaccine Center, Yerkes National Primate Center, Emory University, Atlanta, GA 30322, USA
[5]Division of Infectious Diseases, Department of Medicine, Emory University School of Medicine, Atlanta, GA, USA
[6]Interdisciplinary Graduate Program in Immunology, University of Iowa, Iowa City, IA 52242, USA
[7]Lead Contact
*Correspondence: wendy-maury@uiowa.edu
https://doi.org/10.1016/j.celrep.2020.02.104

SUMMARY

During the 2013–2016 Ebola virus (EBOV) epidemic, a significant number of patients admitted to Ebola treatment units were co-infected with *Plasmodium falciparum,* a predominant agent of malaria. However, there is no consensus on how malaria impacts EBOV infection. The effect of acute *Plasmodium* infection on EBOV challenge was investigated using mouse-adapted EBOV and a biosafety level 2 (BSL-2) model virus. We demonstrate that acute *Plasmodium* infection protects from lethal viral challenge, dependent upon interferon gamma (IFN-γ) elicited as a result of parasite infection. *Plasmodium*-infected mice lacking the IFN-γ receptor are not protected. *Ex vivo* incubation of naive human or mouse macrophages with sera from acutely parasitemic rodents or macaques programs a proinflammatory phenotype dependent on IFN-γ and renders cells resistant to EBOV infection. We conclude that acute *Plasmodium* infection can safeguard against EBOV by the production of protective IFN-γ. These findings have implications for anti-malaria therapies administered during episodic EBOV outbreaks in Africa.

INTRODUCTION

Ebola virus (EBOV) is a negative-strand RNA virus that triggers severe hemorrhagic fever in primates (Feldmann and Geisbert, 2011). EBOV outbreaks, identified sporadically in Central Africa since 1976, cause severe morbidity and mortality, with case fatalities as high as 90% (Weyer et al., 2015). In late 2013, EBOV was detected for the first time in Western Africa, resulting in the largest outbreak in history with 28,600 confirmed cases of EBOV disease (EVD) and a fatality rate of ~40% (Coltart et al., 2017). Given the magnitude of the West African outbreak, multiple epidemiological studies have identified factors that were positively or negatively associated with EVD outcomes. One study reached the conclusion that EBOV patients co-infected with *Plasmodium falciparum*, the principal causative agent of malaria in Africa, were less likely to succumb to EVD, with a survival rates 30% higher in patients with high parasite burdens (Rosenke et al., 2016). In contrast, several additional studies report that *Plasmodium* infection either had no effect on EVD outcomes in pediatric patients or was associated with exacerbated EVD (Smit et al., 2017; Vernet et al., 2017; Waxman et al., 2017). The basis for these disparate conclusions and whether specific host immunity against *Plasmodium* affects either EBOV infection susceptibility or the course of EVD are not fully understood.

The host immune response to *Plasmodium* infection is, in part, governed by the complex life cycle of the parasite and involves multiple tissues (Crompton et al., 2014). The parasite is transmitted into the skin by female *Anopheline* mosquito inoculation of motile sporozoites that results in infection of hepatocytes. These parasites undergo clinically silent differentiation and cell division without triggering robust host cellular immunity. Merozoites are ultimately released from infected hepatocytes and enter a cycle of invasion and asexual replication in red blood cells (RBCs), which elicits the clinical symptoms associated with malarial disease. An initial *Plasmodium* blood-stage infection often stimulates a pro-inflammatory, febrile illness that is associated with elevated interleukin-1β (IL-1β), IL-6, IL-12, interferon gamma (IFN-γ), and tumor necrosis factor (TNF) production (Angulo and Fresno, 2002). In individuals who have either resolved acute febrile illness or have been exposed to repeated *Plasmodium* infections, the immune response shifts to an immunomodulatory profile characterized by IL-10 and transforming growth factor β (TGF-β) production (Portugal et al., 2014). This temporally regulated and functionally dichotomous immune response to *Plasmodium* blood-stage infection provides a possible explanation for the resistance of a subset of *Plasmodium*-infected individuals to EVD and the lack of consensus in the published epidemiological studies of EBOV outbreaks.

Here, we used rodent and non-human-primate models of *Plasmodium*, mouse-adapted EBOV (Mayinga) (ma-EBOV), and a biosafety level 2 (BSL-2) model virus of EBOV to demonstrate that acute *Plasmodium* blood-stage infection protects against EBOV infection and disease. We show that protection conferred

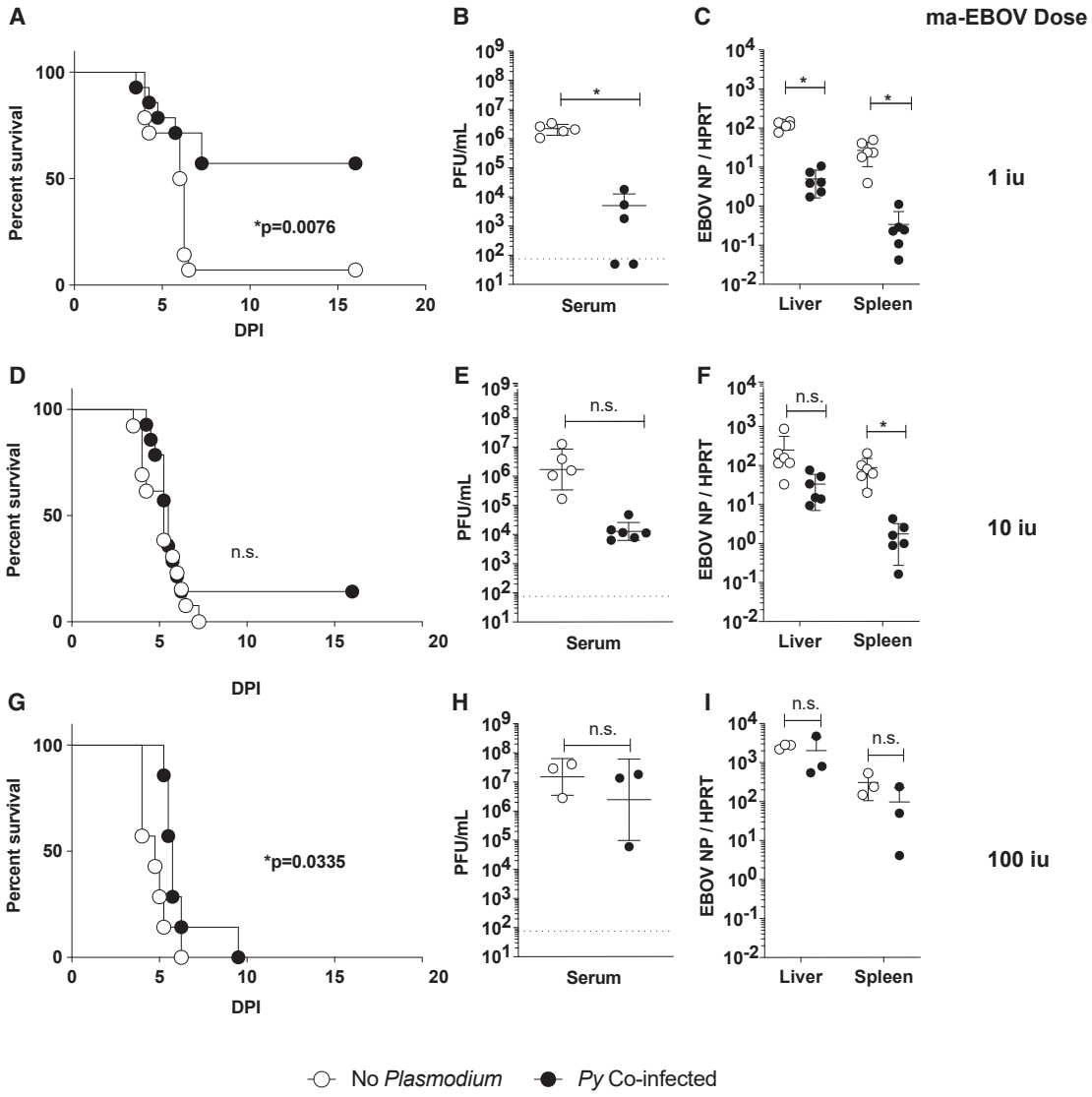

Figure 1. Acute *Plasmodium* Infection in Mice Protects against EBOV Challenge

(A–I) Female BALB/c mice were infected with *Plasmodium yoelii* (*Py*) (1 × 10^6 infected red blood cells [iRBCs]), challenged i.p. 6 days later with 1, 10, or 100 iu mouse-adapted Ebola (ma-EBOV) and assessed for clinical signs and survival daily.

(A, D, and G) Survival curves are shown (n = 14/group in A and D; n = 7/group in G).

(B, E, and H) Day 3 serum titers from individual mice (n = 3–6) are expressed as mean ± SD.

(C, F, and I) Day 3 viral loads in liver and spleen from individual mice (n = 4–6 in B, C, E, and F; n = 3 in H and I) are expressed as mean ± SD.

Experiments in this figure were performed two independent times, and data are pooled (A–F) or once (G–I). For all experiments: n.s., not significant; iu, infectious units; and *p < 0.05.

Also see Figure S1.

by *Plasmodium* is dependent upon IFN-γ production, with loss of IFN-γ signaling abrogating protection.

RESULTS

Acute *Plasmodium* Infection Protects Mice from Lethal ma-EBOV or Recombinant Vesicular Stomatitis Virus (rVSV)/EBOV Glycoprotein (GP) Challenge

To evaluate the effect of an acute *Plasmodium* infection on subsequent EBOV infection, BALB/c mice were intravenously (i.v.) administered RBCs (iRBCs) infected with *Plasmodium yoelii* (17XNL) (*Py*), a rodent *Plasmodium* parasite species that models hyperparasitemia and severe malarial anemia (Li et al., 2001). Six days after *Py* infection, mice were challenged intraperitoneally (i.p.) in a biosafety level 4 (BSL-4) facility with ma-EBOV at a range of infectious doses. At a low, but lethal, dose of 1 infectious unit (iu) of ma-EBOV, *Py*-infected mice exhibited reduced morbidity (Figures S1A and S1B) and mortality (Figure 1A). Consistent with decreased EVD in *Py*-infected mice, serum and organs harvested from the co-infected animals at day 3 of

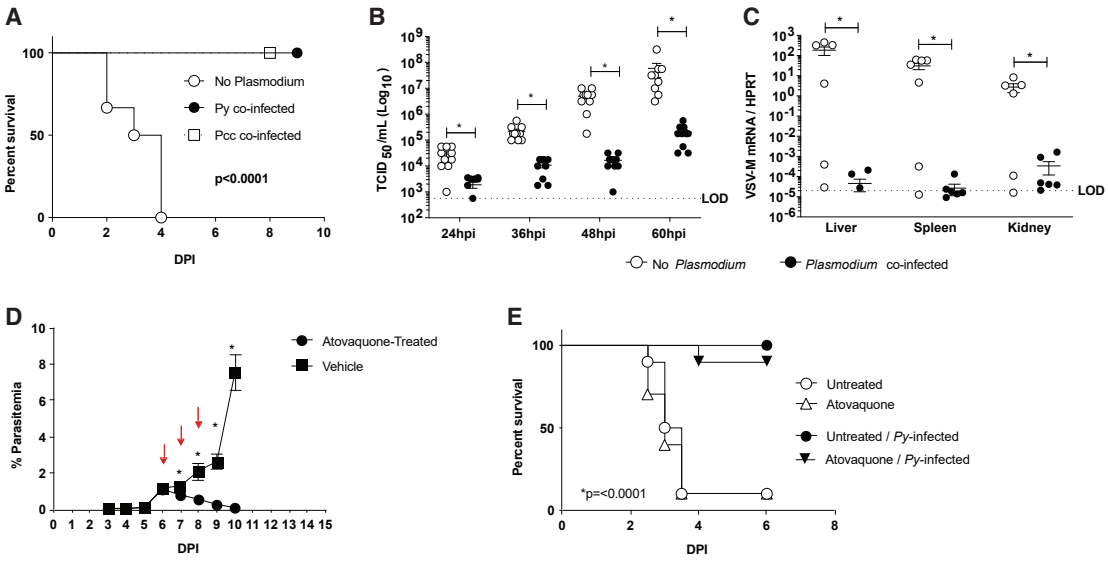

Figure 2. Acute *Plasmodium* Infection of Mice Protects against rVSV/EBOV GP Challenge

(A) C57BL/6 *Ifnar*$^{-/-}$ mice were infected with *Plasmodium yoelii* (*Py*) or *chabaudi* (*Pcc*) (1×10^6 iRBCs) and challenged with rVSV/EBOV GP i.p. 6 days later. Survival curves are shown and analyzed by log-rank (Mantel-Cox) test (n = 12 in no-*Plasmodium* group; n = 11 in *Py*-co-infected group; n = 8 in *Pcc*-co-infected group).

(B and C) C57BL/6 *Ifnar*$^{-/-}$ mice were infected with *Py* or left untreated and challenged with rVSV/EBOV GP i.p. 6 days later. Each point represents a single sample from an individual mouse.

(B) Serum titers at 12-h intervals assessed as tissue culture infectious dose ($TCID_{50}$) $_{per}$ mL on Vero cells.

(C) Viral load in organs at 60 hours post infection (hpi), as assessed by qRT-PCR.

(D and E) C57BL/6 *Ifnar*$^{-/-}$ mice were infected with *Py* or left untreated. Atovaquone was administered to both treatment groups on days 6–8 post-*Py* (red arrows indicate treatments). Parasitemia was monitored daily (n = 10/group).

(D) Mice were infected i.p. with rVSV/EBOV GP on day 9 post-*Py* when the parasite was eradicated in atovaquone-treated mice.

(E) Mice were monitored for survival (n = 10/group).

For all experiments: *p < 0.05. LOD, limit of detection. Error is expressed as mean ± SEM.

Also see Figures S2 and S3.

infection showed a 3-log decrease in viral titers (Figure 1B) and a 1- to 2-log reduction in viral load in the spleen and liver (Figure 1C). Notably, the amount of ma-EBOV administered to mice was critical, as higher doses of virus overcame the protective effect of *Plasmodium in vivo* (Figures 1D–1I), although virus load also trended lower in the *Py*-infected mice administered 10 iu of ma-EBOV.

To explore the mechanisms by which *Py* can protect against ma-EBOV challenge, we used a BSL-2 model of EBOV that challenges IFN-αβ-receptor knockout (*Ifnar*$^{-/-}$) mice with a BSL-2 recombinant rVSV engineered to express the EBOV GP (rVSV/EBOV GP) and green fluorescent protein (GFP) in place of the native GP of VSV. This recombinant virus models EBOV tropism and host cell entry (Takada et al., 1997; Côté et al., 2011; Kondratowicz et al., 2011; Panchal et al., 2014; Wec et al., 2016). Furthermore, infection of *Ifnar*$^{-/-}$ mice with this virus models the effective control of type I IFN responses by EBOV and the *in vivo* and *ex vivo* sensitivity of EBOV to pro-inflammatory and anti-inflammatory cytokines (Takada et al., 1997; Côté et al., 2011; Kondratowicz et al., 2011; Panchal et al., 2014; Rhein et al., 2015; Wec et al., 2016; Rogers et al., 2019). *Ifnar*$^{-/-}$ mice were infected with either *Py* or another rodent *Plasmodium* species, *P. chabaudi chabaudi* (AS) (*Pcc*), which is a model of low-grade parasitemia and persistent malaria (Stephens et al., 2012). When challenged 6 days after establishing either *Py* or *Pcc* infection, mice were protected from an otherwise lethal dose of rVSV/EBOV GP (Figure 2A). In parallel, we found that *Ifnar*$^{-/-}$ mice were not protected from rVSV/EBOV GP when given RBCs from naive mice or irradiated *Py* iRBCs, as previously described (Schmidt et al., 2010) (Figure S2).

Because both *Py* and *Pcc* rendered mice resistant to rVSV/EBOV GP pathogenesis, we conducted subsequent studies by using *Py*, as it more faithfully recapitulates severe acute malarial anemia that would be observed following a primary *Plasmodium* exposure in malaria-naive humans in that it is cleared by the host and does not recrudesce, unlike *Pcc*. Experiments showed that co-infected mice had ~15- to 260-fold lower viremia over the first 60 h of virus infection than mice solely infected with rVSV/EBOV GP (Figure 2B). Similarly, virus loads in the livers, spleens, and kidneys at 60 h of infection were 10^3- to 10^6-fold lower in the *Plasmodium*-infected mice than in non-parasitemic mice, although viral burden was variable in some *Plasmodium*-naive mice (Figure 2C). The low-to-undetectable levels of virus in the peripheral tissues of parasitemic mice at 60 h of infection suggested that virus failed to spread beyond the peritoneal cavity in *Py*-infected animals. At 21 days after virus challenge, half of co-infected mice produced greater than 100 μg/ml of anti-EBOV GP antibodies, immunoglobulin

(Ig) concentrations that we previously showed to be protective against subsequent ma-EBOV challenge (Figure S3) (Lennemann et al., 2017). Less than 1 μg/ml of anti-EBOV GP Ig was detected in some of rVSV/EBOV GP-challenged mice, suggesting either that virus titers were insufficient to elicit a significant humoral response in these animals or *Py* infection interfered with anti-EBOV GP antibody production. Together, these data show that an active blood-stage *Plasmodium* infection protects mice from challenge with lethal doses of either ma-EBOV or rVSV/EBOV GP. Importantly, the rVSV/EBOV GP experimental system using an *Ifnar*$^{-/-}$ host excludes a role for type 1 IFN signaling in the protection conferred by *Plasmodium* infection.

To determine whether parasite infection was directly facilitating protection, we infected mice with *Py* and, on days 6–8 post-inoculation (p.i.), administered the anti-malarial drug atovaquone to parasitemic and naive control mice. Parasitemia was quantified daily, and mice were challenged with rVSV/EBOV GP upon successful eradication of *Py* (Figure 2D). Strikingly, *Py*-infected mice treated with atovaquone remained protected from rVSV/EBOV GP, suggesting that the protection against lethal virus challenge mediated by acute *Py* infection was more likely to be due to the host immune response rather than the presence of the parasite per se (Figure 2E). Notably, atovaquone treatment did not impact the disease course in *Plasmodium* naive mice.

Peritoneal Macrophages Are Crucial for *Plasmodium*-Elicited Protection from rVSV/EBOV GP

EBOV is primarily a myeloid cell-tropic pathogen (Connolly et al., 1999; Geisbert et al., 2003; Bray and Geisbert, 2005; Rogers and Maury, 2018), and peritoneal macrophages (pmacs) are the primary cell population initially infected during i.p. administration of maEBOV or rVSV/EBOV GP (Mahanty et al., 2003; Rhein et al., 2015; Rogers et al., 2019). To address whether acute experimental malaria impacts virus infection of these critical target cells, *Py*-infected and naive mice were challenged i.p. with rVSV/EBOV GP. Peritoneal cells were harvested at 24 h and assessed for viral load. Although most naive mice showed high levels of viral RNA in peritoneal cells, virus was largely undetectable in cells recovered from *Py*-infected mice (Figure 3A, left). Consistent with these *in vivo* data, *ex vivo* virus challenge of pmacs that were obtained from *Py*-infected mice and enriched by adherence showed a ~30-fold decrease in viral load at 24 h of infection compared with pmacs obtained from naive mice (Figure 3A, right). These data support that *in vivo Py* infection restricts viral infection of a primary cell target of EBOV, pmacs, despite the fact that *Py* merozoites do not infect macrophages but specifically target RBCs.

The studies with an anti-malarial agent demonstrating that mice cleared of *Py*-infected RBCs remained protected against virus challenge raised the possibility that the host inflammatory responses to blood-stage *Plasmodium* infection may program resistance to ma-EBOV and rVSV/EBOV GP infection. To test this, we incubated pmacs from naive donors with dose titrations of serum from either *Py*-infected or naive mice for 24 h and then challenged the cells with wild-type EBOV or rVSV/EBOV GP. Serum from *Py*-infected animals protected pmacs from virus infection in a dose-dependent manner (Figures 3B and 3C).

We previously showed that IFN-γ can protect macrophages from EBOV infection (Rhein et al., 2015). Thus, we postulated that *Plasmodium*-induced IFN-γ is mechanistically linked to *Plasmodium*-infection-induced protection against EBOV and rVSV/EBOV GP challenge that was observed both *in vivo* and *ex vivo*. In support of this, serum levels of IFN-γ were markedly elevated as early as 4 days after *Py* infection in *Ifnar*$^{-/-}$ and wild-type mice, peaking at day 6, whereas no detectable IFN-γ was observed in naive serum (Figure 3D; Figure S4A). In line with these elevated serum IFN-γ levels, transcriptional changes in pmacs recovered from *Py*-infected mice exhibited a proinflammatory macrophage M1 phenotype characterized by enhanced expression of the well-established IFN stimulated genes (ISGs) *IRF1* and *GBP5* (Figure 3E). Similarly, the addition of serum from *Py*-infected donors stimulated dose-dependent increases in IRF1 and GPB5 expression in pmacs harvested from naive mice (Figure 3F). Importantly, the *ex vivo* protective effects of serum from *Py*-infected donors was abolished by neutralizing IFN-γ (Figure 3G).

To extend these studies to a model that more directly approximates human *Plasmodium* infection, we next evaluated the capacity of serum obtained from rhesus macaques acutely infected with *Plasmodium cynomolgi* (Collins et al., 1999) to program virus resistance in human monocyte-derived macrophages (MDMs), as many human and non-human primate (NHP) cytokines are known to cross react (Scheerlinck, 1999). Consistent with the results from our rodent studies, viral replication was 20- to 30-fold lower in the MDMs exposed to serum from acutely *Plasmodium*-infected macaques (Figure 3H, left). Serum exposure also elevated M1 markers associated with IFN-γ signaling (Figure 3H, right). Collectively, these data suggest that IFN-γ produced in response to acute *Plasmodium* infection protects human and mouse macrophages from EBOV infection.

Plasmodium-Elicited IFN-γ Production Is Necessary for *In Vivo* Protection from rVSV/EBOV GP

We next sought to determine if IFN-γ signaling was responsible for the *in vivo* protection mediated by *Py* infection. To test this, we infected IFN-γ-receptor-null (*Ifngr1*$^{-/-}$) mice with *Py* and isolated serum and pmacs 6 days after establishing blood-stage *Plasmodium* infection (Figure 4A). The pmacs of *Py*-infected and naive *Ifngr1*$^{-/-}$ mice showed no difference in levels of infection upon rVSV/EBOV GP challenge and exhibited no evidence of M1 polarization (Figure 4B). However, *Ifngr1*$^{-/-}$ mice retained the capacity to secrete IFN-γ, as *Ifnar*$^{-/-}$ pmacs exposed to the serum of *Py*-infected *Ifngr1*$^{-/-}$ animals exhibited reduced viral loads and expressed the M1-polarized ISGs *IRF-1* and *GBP5* (Figure 4C). To evaluate the role of IFN-γ signaling *in vivo*, we generated and infected *Ifnar*$^{-/-}$*Ifngr1*$^{-/-}$ mice with *Plasmodium.* Double-knockout mice were used, as VSV-based recombinant viruses are not virulent in mice with intact IFNAR signaling due to an inability to antagonize type I IFN (Müller et al., 1994). We found that *Ifnar*$^{-/-}$*Ifngr1*$^{-/-}$ mice produced robust levels of IFN-γ when exposed to *Py* (Figure S4B) but were not protected from rVSV/EBOV GP challenge (Figure 4D). Although parasitemia during early *Py* and *Pcc* infection of *Ifngr1*$^{-/-}$ mice has been shown to be elevated compare to wild-type mice (Su and Stevenson, 2000), the *Py* parasite burden of *Ifnar*$^{-/-}$*Ifngr1*$^{-/-}$ mice did not alter their survival if these mice were not challenged with virus (Figure 4D). Virus infection of these mice resulted in higher systemic viremia at 24 h and 48 h than virus-challenged

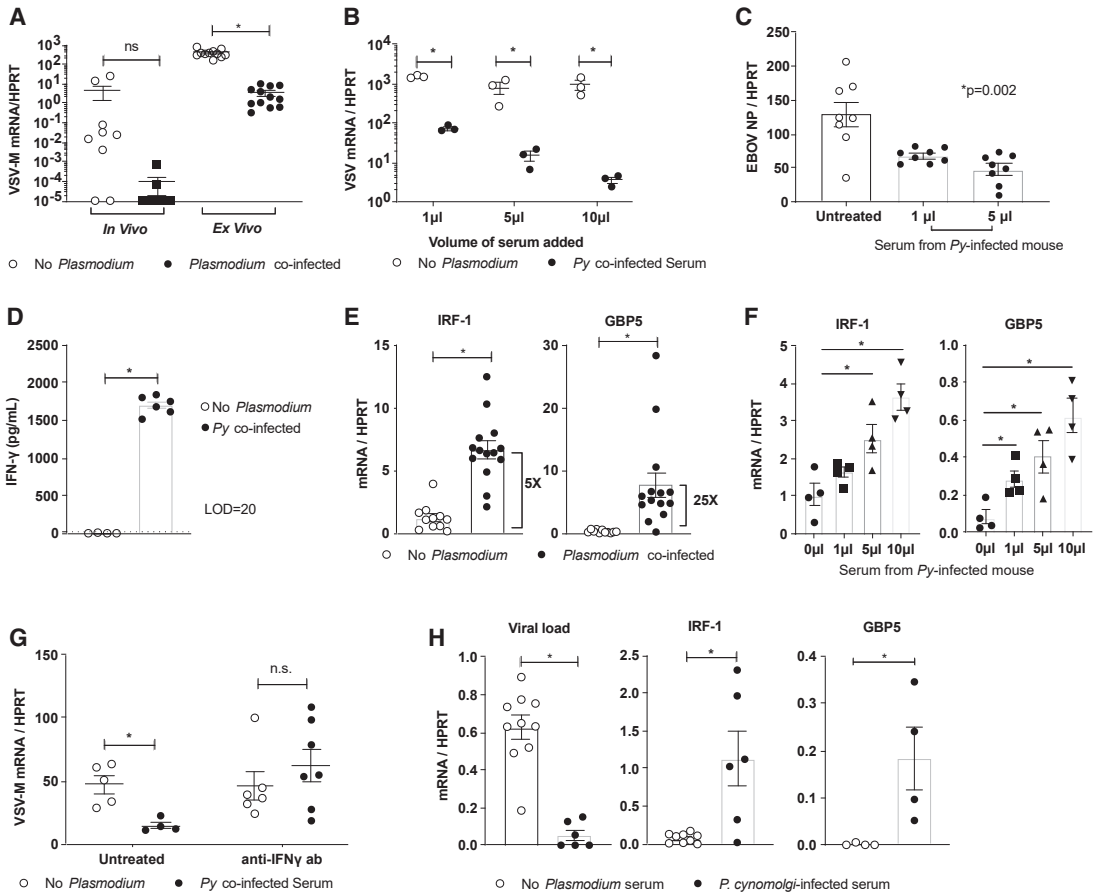

Figure 3. Peritoneal Macrophages Are Critical Mediators of *Plasmodium*-Elicited Protection from rVSV/EBOV GP

(A–G) C57BL/6 *Ifnar*$^{-/-}$ mice were inoculated with 1 × 10^6 *Py* iRBCs or left untreated, and all experiments were performed 6 days after *Py* was administered.

(A) For *in vivo* infections, mice were challenged with a lethal dose of rVSV/EBOV GP, pmacs were harvested at 24 hpi, and viral replication was assessed by qRT-PCR (*in vivo*). For *ex vivo* infections, pmacs were harvested from mice, infected with rVSV/EBOV GP (multiplicity of infection [MOI] = 1), and assessed by qRT-PCR at 24 hpi (*ex vivo*).

(B) Pmacs from naive mice were harvested, treated for 24 h with serum from either naive mice or *Py*-infected mice, and infected with rVSV/EBOV GP (MOI = 1). Viral loads were assessed 24 hpi.

(C) Pmacs were treated with serum from *Py*-infected mice and infected with wild-type (WT) EBOV under BSL-4 conditions. Infection was quantified by qRT-PCR for EBOV NP gene expression at 24 hpi.

(D) IFN-γ levels in serum on day 6 were assessed by ELISA.

(E and F) M1 polarization markers were assessed in untreated or *Py*-infected serum exposed pmacs by qRT-PCR (E). A dose-response curve of *Py*-infected serum added to pmacs (F).

(G) Pmacs exposed to *Py*-infected serum in the presence or absence of anti-IFN-γ antibody for 24 h and then infected with rVSV/EBOV GP (MOI = 1). Infection was assessed by qRT-PCR 24 hpi.

(H) Human MDMs were incubated with serum from *Cynomolgous* macaques infected with *Plasmodium cynomolgi*. Cells were challenged with rVSV/EBOV GP (MOI = 5), and infection was quantified at 24 hpi by qRT-PCR. Uninfected pmacs treated with serum from naive or *P. cynomolgi*-infected macaques were assessed for M1 polarization markers by qRT-PCR.

For all experiments: *$p < 0.05$. Error is expressed as mean ± SEM.

Also see Figure S4.

naive *Ifnar*$^{-/-}$*Ifngr1*$^{-/-}$ mice (Figure 4E) and higher viral loads in the liver but lower loads in the spleen (Figure 4F), suggesting that, in the absence of type II IFN signaling, acute *Py* infection enhances overall virus load. Moreover, neither *Py*-infected mouse serum nor recombinant IFN-γ protected *Ifngr1*$^{-/-}$ pmacs against challenge with the BSL-4 EBOV (Mayinga) (Figure 4G).

Finally, we sought to determine the cells responsible for IFN-γ production due to *Py* infection. As it has been reported that both natural killer (NK) cells and T cells are the source of IFN-γ (De Souza et al., 1997; Villegas-Mendez et al., 2012; King and Lamb, 2015), we performed cell-depletion studies and found that T cells, but not NK cells, are critical for *Py*-mediated protection from rVSV/EBOV GP (Figure 4H). Together, these data support that IFN-γ and its interactions with the IFN-γ receptor are critical for *Plasmodium*-mediated protection against EBOV infection.

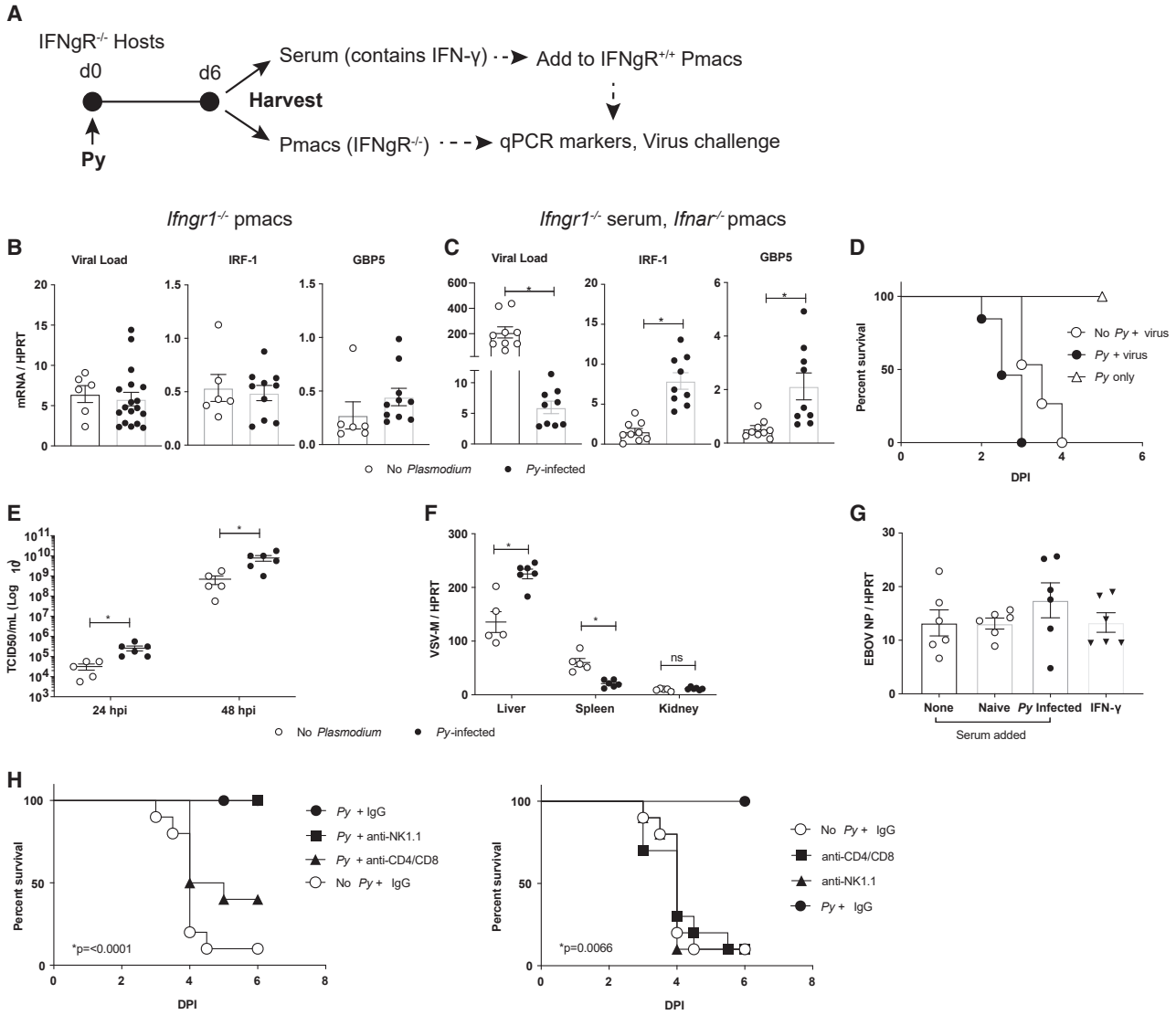

Figure 4. *Plasmodium*-Dependent Protection against EBOV and rVSV/EBOV GP Requires IFN-γ/IFN-γR Interactions

(A–C) Pmacs from *Ifngr1*$^{-/-}$ mice are not protected against rVSV/EBOV GP. *Ifngr1*$^{-/-}$ mice were inoculated with 1 × 10^6 *Py* iRBCs or left untreated, and 6 days later, sera and pmacs were harvested and cells were infected *ex vivo*.

(A) A schematic of the experiment.

(B) Parasitemic or naive *Ifngr1*$^{-/-}$ pmacs were infected *ex vivo* with rVSV/EBOV GP (MOI = 5), and infection was quantified at 24 hpi or left uninfected and assessed for expression of M1 markers.

(C) Serum from *Ifngr1*$^{-/-}$ mice was added to *Ifnar*$^{-/-}$ pmacs for 24 h. Cells were either infected *ex vivo* with rVSV/EBOV GP (MOI = 1) with infection quantified at 24 hpi by qRT-PCR or left uninfected and assessed for expression of M1 markers.

(D–F) *Ifnar/Ifngr1*$^{-/-}$ mice were inoculated with either 1 × 10^6 Py iRBCs or left untreated and 6 days later challenged i.p. with a lethal dose of rVSV/EBOV GP.

(D) Survival curves following virus challenge (n = 15 in no Py + virus group; n = 13 in Py + virus group; n = 3 in Py-only group).

(E) Serum virus titers at 24 and 48 hpi.

(F) Viral loads in organs harvested 48 hpi.

(G) *Ifngr1*$^{-/-}$ pmacs were treated as shown and infected with WT EBOV under BSL-4 conditions, and infection was quantified by qRT-PCR for EBOV NP gene expression at 24 hpi.

(H) C57BL/6 *Ifnar*$^{-/-}$ mice were infected with Py (1 × 10^6 iRBCs), treated with 200 μg of the indicated antibodies 24 hpi, and challenged with rVSV/EBOV GP i.p. on day 6 post-infection. The x axis represents days following virus challenge. Survival was monitored (n = 10/group). Controls are included as a separate panel (right) to facilitate interpretation.

For all experiments: *p < 0.05. Error is expressed as mean ± SEM.

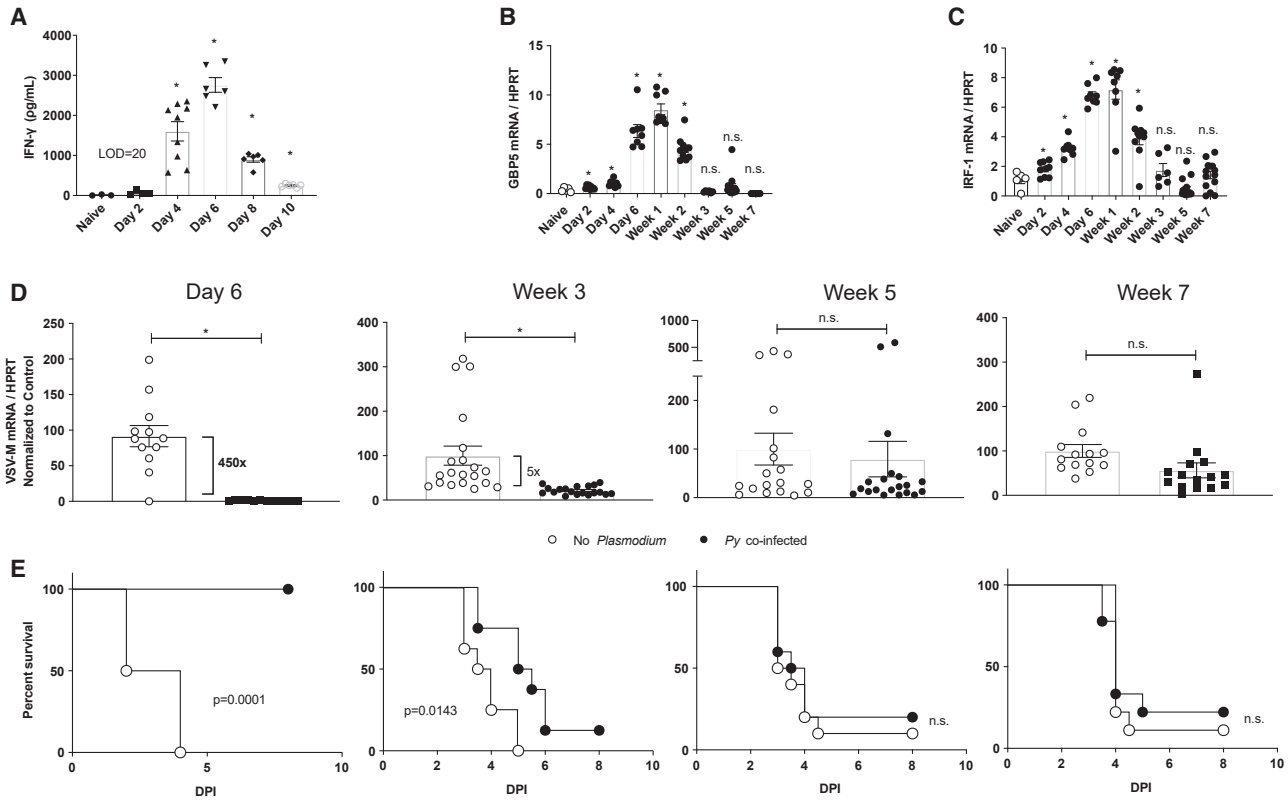

Figure 5. Durability of *Plasmodium*-Mediated Protection to rVSV/EBOV GP

For all experiments, C57BL/6 *Ifnar*$^{-/-}$ mice were inoculated with 1 × 10^6 *Py* iRBCs or left untreated. All experiments were performed at the indicated time after *Py* infection.

(A) Serum was harvested and IFN-γ levels were quantified by ELISA.

(B and C) Pmacs were harvested, RNA was isolated, and expression of GBP5 (B) and IRF-1 (C) was quantified by qRT-PCR.

(D) Pmacs were harvested at times noted and infected *ex vivo* with rVSV/EBOV GP (MOI = 1). Virus infection was quantified 24 hpi by qRT-PCR.

(E) Mice were challenged i.p. with a lethal dose of rVSV/EBOV GP (n = 8–10) at times noted in (D).

For all experiments: *p < 0.05. Error is expressed as mean ± SEM.

Also see Figure S5.

Plasmodium-Elicited Protection from rVSV/EBOV GP Wanes over Time

Given that the host response to acute blood-stage *Plasmodium* infection evolves from pro-inflammatory to immunomodulatory after resolution of infection, we evaluated the durability of *Py*-infection-induced protection against rVSV/EBOV GP challenge. IFN-γ in the serum of *Py*-infected *Ifnar*$^{-/-}$ mice peaked on day 6 p.i. and fell below the limit of detection after day 10 p.i. (Figure 5A). In contrast, M1 markers on pmacs recovered from *Py*-infected mice remained upregulated after IFN-γ was no longer detectable in peripheral blood (Figures 5B and 5C). To probe the relationship between IFN-γ-induced M1 pmac polarization and protection against virus challenge, we isolated pmacs at weeks 1, 3, 5, and 7 following *Py* infection and challenged the cells with rVSV/EBOV GP *ex vivo*. In parallel experiments designed to evaluate the durability of *in vivo* protection, we also challenged *Py*-infected mice at weeks 1, 3, 5, and 7 following *Py* infection with rVSV/EBOV GP. Strikingly, both *Py*-infected mice and pmacs harvested from *Py*-infected mice were protected from virus challenge for 3 weeks, but protection waned by 5 weeks after *Py* infection (Figures 5D and 5E). Thus, the *in vivo* and *ex vivo* consequences of M1 polarization due to experimental *Py* infection of the *Ifnar*$^{-/-}$ host persist for at least 3 weeks. Notably, administration of a single high dose of recombinant IFN-γ only protected mice when administered within 24 h of rVSV/EBOV challenge (Figure S5A), suggesting that either persistent, sub-patent *Plasmodium* infection and/or sustained, low-grade IFN-γ production imprints more strongly on macrophages than a single bolus of recombinant cytokine. Indeed, the protective effects of recombinant IFN-γ were abrogated when mice were challenged with a 10- to 100-fold higher dose of rVSV/EBOV GP (Figure S5B). Similarly, IFN-γ did not provide protection to pmacs challenged with a 10-fold higher dose of wild-type EBOV (Figure S5C**)**. These data are consistent with our *in vivo* ma-EBOV findings (Figure 1) and recent reports from others (Rosenke et al., 2018) showing that experimental malaria fails to modulate the course of EVD when mice are challenged with large doses (eg, 100 lethal dose 50 [LD_{50}]) of ma-EBOV.

DISCUSSION

Our studies demonstrate that acute infection with *Plasmodium* transiently protects mice from EBOV challenge. Our findings in mice support the epidemiological study by Rosenke et al. (2016) that observed that during the 2013–2016 EBOV outbreak, overt *Plasmodium* infection was associated with protection against disease symptoms and fatalities associated with EBOV infection. We elucidated the mechanism by which *Plasmodium* facilitates protection against EBOV, identifying that *Plasmodium* infection stimulates IFN-γ production, with serum levels peaking at day 6 following *Plasmodium* infection. This pro-inflammatory environment polarized tissue macrophages, resulting in inhibition of virus infection. Eliminating IFN-γ/IFNgR interactions abrogated the protection conferred by *Plasmodium* against rVSV/EBOV GP, strengthening the mechanistic link. We previously reported that IFN-γ administration abrogates virus infection of pmacs and protects mice from an otherwise lethal challenge with ma-EBOV or rVSV/EBOV GP (Rhein et al., 2015), which is consistent with our *ex vivo* BSL-4 data demonstrating a dependence on IFN-γ production. The data presented here further implicate IFN-γ as a potential EBOV antiviral as a therapeutic strategy at early times of virus infection.

Our findings demonstrate that acute *Plasmodium* infection generates sufficient IFN-γ to protect against a low, but uniformly lethal, dose of EBOV; however, we found that it is not protective against higher EBOV doses. The inability of *Py* infection to overcome higher doses of EBOV is consistent with an earlier report that showed that *Py* infection does not alter morbidity or mortality associated with the administration of 100 LD_{50} of EBOV to mice (Rosenke et al., 2018). Recombinant IFN-γ administration also protected against low doses, but not high doses, of rVSV/EBOV GP in *Ifnar*$^{-/-}$ mice, in a manner similar to protection conferred by acute *Py* in ma-EBOV studies. These studies provide supporting evidence that our BSL-2 model virus serves as an appropriate model system for dissecting these mechanisms of protection against EVD. Acceptance of BSL-2 models overcomes space and cost restrictions associated with BSL-4 studies.

An important question that bears on the relevance of our studies and others is what is the dose of EBOV to which individuals are likely to be exposed? Furthermore, what dose of virus is required for an individual to become viremic and manifest symptoms? Although answers to these questions are not known, as we show here, the use of a low but predictably lethal dose in an animal model can provide important insight and understanding into the ability of the immune system to successfully overcome these highly virulent infections under some conditions. Additionally, such doses may more accurately reflect exposure within the field.

Some epidemiological studies from the 2013–2016 outbreak found that co-infection with *Plasmodium* enhanced EVD (Smit et al., 2017; Vernet et al., 2017; Waxman et al., 2017). We propose that these conclusions were drawn from studies that lack adequate stratification of malaria-infected patients based on cytokine profiles. It is well-established that immune responses to acute versus chronic (or repeated) *Plasmodium* infections differ. Although an acute *Plasmodium* challenge of a naive individual is known to elicit a strong type 1 immune response, subsequent or chronic infection of an individual shifts the immune response to an anti-inflammatory type 2 response (Angulo and Fresno, 2002). Thus, many parasitemic patients in endemic regions have sub-clinical infections with elevated levels of TGF-β and IL-10 and an absence of pro-inflammatory cytokines (Portugal et al., 2014). As a consequence, the presence or absence of parasites in the blood of patients entering an Ebola treatment unit (ETU) may be an insufficient clinical marker to predict the severity and clinical course of EVD. Instead, serum cytokine profiles may better serve as a predictor of outcome. Hence, our studies suggest that it would be valuable for clinical protocols in ETUs to distinguish *Plasmodium*-infected patients by their cytokine profile. Although such clinical tests may currently be difficult to perform in resource-poor regions, the current approach of treating all RBC *Plasmodium*-positive individuals in ETUs may reduce beneficial pro-inflammatory cytokines present at early times in some EBOV-infected patients.

To control for pre-exposure and *Plasmodium* infection timelines and data, we chose to work with two animal models of acute *Plasmodium* infection. The results of longitudinal serum draws from *Py*-infected mice challenged with rVSV/EBOV GP indicate that *Py*-infected mice become viremic, albeit at much lower levels than *Py*-naive mice, and that some of these mice develop a robust antibody response to EBOV GP following virus challenge. However, other mice in this treatment group produced few to no detectable anti-EBOV GP antibodies, suggesting that the virus antigens in those mice may have been insufficient to stimulate a humoral response or that *Plasmodium* co-infection blocked antibody development, as has been suggested by others (Muellenbeck et al., 2013; Scholzen and Sauerwein, 2013).

Evidence of EBOV GP antibody seropositivity in the absence of clinical disease provides potential insights into recent reports that have identified a surprising number of individuals in sub-Saharan Africa who have no known contact with EBOV and, yet, are seropositive for anti-EBOV antibodies. Recent estimates range from 0%–24% of patient populations (Mulangu et al., 2016; Bower and Glynn, 2017; Steffen et al., 2019). Given the pervasive presence of malaria in regions where EBOV is endemic, *Plasmodium*-elicited subclinical co-infections with EBOV may occur, resulting in a small percentage of seropositive individuals who may be protected against subsequent EBOV infection.

The effects of IFN-γ on macrophages, and the resulting M1 phenotype it induced, lasted several weeks. Although the peak production of IFN-γ occurred at day 6, M1 markers remained elevated for an additional week, with intermediate levels of protection in mice and macrophages observed up to 2 weeks later. This is of interest, as little has been done to investigate the durability of the phenotypes induced by polarizing agents in primary macrophages or *in vivo*. Furthermore, the absolute levels of IFN-γ achieved in the serum during *Plasmodium* infection are much lower than the dose we had previously administered directly to the peritoneal cavity to elicit protection (Rhein et al., 2015); yet, they were protective. This could indicate that lower levels of sustained IFN-γ have a long-lasting protective effect, allowing for lower doses administered and, thus, more desirable side effect profiles. Although it is difficult to compare the production of

cytokines such as IFN-γ across taxa from mice to humans, numerous groups have shown that human patients produce large amounts of IFN-γ in response to *Plasmodium* infection, and the role of IFN-γ during clinical malaria is well characterized (Rhodes-Feuillette et al., 1985; Medina et al., 2011; Perlaza et al., 2011; Nasr et al., 2014; King and Lamb, 2015). For instance, Medina et al. (2011) report a range of serum IFN-γ levels from 30 to 76 ng/ml in humans acutely infected with *Plasmodium vivax*.

Taken together, these data indicate that acute *Plasmodium* infection protects against EBOV infection in a mouse model by eliciting the production of IFN-γ. Furthermore, our rVSV/EBOV GP studies demonstrated that IFN-γ signaling through IFNgR is required for this protection. This leads to pro-inflammatory polarization of macrophages that restricts EBOV replication in key cell populations. Future studies to examine additional IFN-γ signaling requirements and downstream IFN-stimulated genes mediating IFN-γ effects would further our understanding of this protection. An earlier study demonstrated that *Py* infection protects mice against acute chikungunya virus viremia and pathology in an IFN-γ-dependent manner (Teo et al., 2018). This argues that *Plasmodium*-elicited proinflammatory responses may inhibit a variety of acute viral infections. In combination, these findings suggest that similar studies in virus-infected NHP models are warranted to determine if protection would translate to humans. Furthermore, re-evaluation of the current strategy of administration of anti-malarial therapeutics upon all parasitemic patients at ETUs may be warranted.

STAR★METHODS

Detailed methods are provided in the online version of this paper and include the following:

- KEY RESOURCES TABLE
- LEAD CONTACT AND MATERIALS AVAILABILITY
- EXPERIMENTAL MODEL AND SUBJECT DETAILS
  - Mice
  - Nonhuman primate Plasmodium cynomolgi infections
  - rVSV/EBOV GP stocks
  - WT EBOV stocks
  - Plasmodium infections and parasite quantification
- METHOD DETAILS
  - BSL-4 mouse experiments
  - BSL-2 mouse experiments
  - Titer assay (BSL-2)
  - Organ Harvest
  - qRT-PCR
  - ELISAs
  - Serum isolation and *ex vivo* treatments
  - Macrophage isolations
- QUANTIFICATION AND STATISTICAL ANALYSIS
- DATA AND CODE AVAILABILITY

SUPPLEMENTAL INFORMATION

Supplemental Information can be found online at https://doi.org/10.1016/j.celrep.2020.02.104.

ACKNOWLEDGMENTS

This study was supported by AI139902 to W.M. N.S.B. also was supported by the NIH grant numbers AI125446 and AI127481. M.R.G. and C.J.J. were supported by NIH/NIAID contract number HHSN272201200031C and NIH Office of Research Infrastructure Programs/OD P51OD011132. K.J.R. was supported by NIH training grants T32 GM007337 and T32 GM 067795. Analyses were confirmed by the Institute for Clinical and Translational Science Biostatistics Core that was supported by NIH UL1TR002537.

AUTHOR CONTRIBUTIONS

Conceptualization, K.J.R., N.S.B., and W.M.; Methodology, K.J.R., O.S., R.V., C.J.J., M.R.G., N.S.B., and W.M.; Investigation, K.J.R., O.S., R.V., and L.N.M.; Writing – Original Draft, K.J.R.; Writing – Review & Editing, K.J.R., O.S., R.V., C.J.J., M.R.G., N.S.B., and W.M.; Funding Acquisition, N.S.B. and W.M.; Resources, N.S.B. and W.M.; Supervision, W.M.

DECLARATION OF INTERESTS

The authors declare no competing interests.

Received: August 30, 2019
Revised: January 6, 2020
Accepted: February 27, 2020
Published: March 24, 2020

REFERENCES

Angulo, I., and Fresno, M. (2002). Cytokines in the pathogenesis of and protection against malaria. Clin. Diagn. Lab. Immunol. *9*, 1145–1152.

Bower, H., and Glynn, J.R. (2017). A systematic review and meta-analysis of seroprevalence surveys of ebolavirus infection. Sci. Data *4*, 160133.

Bray, M., and Geisbert, T.W. (2005). Ebola virus: the role of macrophages and dendritic cells in the pathogenesis of Ebola hemorrhagic fever. Int. J. Biochem. Cell Biol. *37*, 1560–1566.

Bray, M., Davis, K., Geisbert, T., Schmaljohn, C., and Huggins, J. (1998). A mouse model for evaluation of prophylaxis and therapy of Ebola hemorrhagic fever. J. Infect. Dis. *178*, 651–661.

Collins, W.E., Warren, M., and Galland, G.G. (1999). Studies on infections with the Berok strain of *Plasmodium cynomolgi* in monkeys and mosquitoes. J. Parasitol. *85*, 268–272.

Coltart, C.E., Lindsey, B., Ghinai, I., Johnson, A.M., and Heymann, D.L. (2017). The Ebola outbreak, 2013-2016: old lessons for new epidemics. Philos. Trans. R. Soc. Lond. B Biol. Sci. *372*, 20160297.

Connolly, B.M., Steele, K.E., Davis, K.J., Geisbert, T.W., Kell, W.M., Jaax, N.K., and Jahrling, P.B. (1999). Pathogenesis of experimental Ebola virus infection in guinea pigs. J. Infect. Dis. *179* (*Suppl 1*), S203–S217.

Côté, M., Misasi, J., Ren, T., Bruchez, A., Lee, K., Filone, C.M., Hensley, L., Li, Q., Ory, D., Chandran, K., and Cunningham, J. (2011). Small molecule inhibitors reveal Niemann-Pick C1 is essential for Ebola virus infection. Nature *477*, 344–348.

Crompton, P.D., Moebius, J., Portugal, S., Waisberg, M., Hart, G., Garver, L.S., Miller, L.H., Barillas-Mury, C., and Pierce, S.K. (2014). Malaria immunity in man and mosquito: insights into unsolved mysteries of a deadly infectious disease. Annu. Rev. Immunol. *32*, 157–187.

De Souza, J.B., Williamson, K.H., Otani, T., and Playfair, J.H. (1997). Early gamma interferon responses in lethal and nonlethal murine blood-stage malaria. Infect. Immun. *65*, 1593–1598.

Ebihara, H., Theriault, S., Neumann, G., Alimonti, J.B., Geisbert, J.B., Hensley, L.E., Groseth, A., Jones, S.M., Geisbert, T.W., Kawaoka, Y., and Feldmann, H. (2007). *In vitro* and *in vivo* characterization of recombinant Ebola viruses expressing enhanced green fluorescent protein. J. Infect. Dis. *196* (*Suppl 2*), S313–S322.

Feldmann, H., and Geisbert, T.W. (2011). Ebola haemorrhagic fever. Lancet *377*, 849–862.

Geisbert, T.W., Hensley, L.E., Larsen, T., Young, H.A., Reed, D.S., Geisbert, J.B., Scott, D.P., Kagan, E., Jahrling, P.B., and Davis, K.J. (2003). Pathogenesis of Ebola hemorrhagic fever in cynomolgus macaques: evidence that dendritic cells are early and sustained targets of infection. Am. J. Pathol. *163*, 2347–2370.

Joyner, C., Moreno, A., Meyer, E.V., Cabrera-Mora, M., Kissinger, J.C., Barnwell, J.W., and Galinski, M.R.; MaHPIC Consortium (2016). *Plasmodium cynomolgi* infections in rhesus macaques display clinical and parasitological features pertinent to modelling vivax malaria pathology and relapse infections. Malar. J. *15*, 451.

King, T., and Lamb, T. (2015). Interferon-γ: The Jekyll and Hyde of Malaria. PLoS Pathog. *11*, e1005118.

Kondratowicz, A.S., Lennemann, N.J., Sinn, P.L., Davey, R.A., Hunt, C.L., Moller-Tank, S., Meyerholz, D.K., Rennert, P., Mullins, R.F., Brindley, M., et al. (2011). T-cell immunoglobulin and mucin domain 1 (TIM-1) is a receptor for Zaire Ebolavirus and Lake Victoria Marburgvirus. Proc. Natl. Acad. Sci. USA *108*, 8426–8431.

Lennemann, N.J., Herbert, A.S., Brouillette, R., Rhein, B., Bakken, R.A., Perschbacher, K.J., Cooney, A.L., Miller-Hunt, C.L., Ten Eyck, P., Biggins, J., et al. (2017). Vesicular Stomatitis Virus Pseudotyped with Ebola Virus Glycoprotein Serves as a Protective, Noninfectious Vaccine against Ebola Virus Challenge in Mice. J. Virol. *91*, e00479-17.

Li, C., Seixas, E., and Langhorne, J. (2001). Rodent malarias: the mouse as a model for understanding immune responses and pathology induced by the erythrocytic stages of the parasite. Med. Microbiol. Immunol. (Berl.) *189*, 115–126.

Mahanty, S., Gupta, M., Paragas, J., Bray, M., Ahmed, R., and Rollin, P.E. (2003). Protection from lethal infection is determined by innate immune responses in a mouse model of Ebola virus infection. Virology *312*, 415–424.

Malleret, B., Claser, C., Ong, A.S., Suwanarusk, R., Sriprawat, K., Howland, S.W., Russell, B., Nosten, F., and Rénia, L. (2011). A rapid and robust tri-color flow cytometry assay for monitoring malaria parasite development. Sci. Rep. *1*, 118.

Medina, T.S., Costa, S.P., Oliveira, M.D., Ventura, A.M., Souza, J.M., Gomes, T.F., Vallinoto, A.C., Póvoa, M.M., Silva, J.S., and Cunha, M.G. (2011). Increased interleukin-10 and interferon-γ levels in *Plasmodium vivax* malaria suggest a reciprocal regulation which is not altered by IL-10 gene promoter polymorphism. Malar. J. *10*, 264.

Muellenbeck, M.F., Ueberheide, B., Amulic, B., Epp, A., Fenyo, D., Busse, C.E., Esen, M., Theisen, M., Mordmüller, B., and Wardemann, H. (2013). Atypical and classical memory B cells produce *Plasmodium falciparum* neutralizing antibodies. J. Exp. Med. *210*, 389–399.

Mulangu, S., Borchert, M., Paweska, J., Tshomba, A., Afounde, A., Kulidri, A., Swanepoel, R., Muyembe-Tamfum, J.J., and Van der Stuyft, P. (2016). High prevalence of IgG antibodies to Ebola virus in the Efé pygmy population in the Watsa region, Democratic Republic of the Congo. BMC Infect. Dis. *16*, 263.

Müller, U., Steinhoff, U., Reis, L.F., Hemmi, S., Pavlovic, J., Zinkernagel, R.M., and Aguet, M. (1994). Functional role of type I and type II interferons in antiviral defense. Science *264*, 1918–1921.

Nasr, A., Allam, G., Hamid, O., and Al-Ghamdi, A. (2014). IFN-gamma and TNF associated with severe falciparum malaria infection in Saudi pregnant women. Malar. J. *13*, 314.

Panchal, R.G., Mourich, D.V., Bradfute, S., Hauck, L.L., Warfield, K.L., Iversen, P.L., and Bavari, S. (2014). Induced IL-10 splice altering approach to antiviral drug discovery. Nucleic Acid Ther. *24*, 179–185.

Perlaza, B.L., Sauzet, J.P., Brahimi, K., BenMohamed, L., and Druilhe, P. (2011). Interferon-γ, a valuable surrogate marker of *Plasmodium falciparum* pre-erythrocytic stages protective immunity. Malar. J. *10*, 27.

Portugal, S., Moebius, J., Skinner, J., Doumbo, S., Doumtabe, D., Kone, Y., Dia, S., Kanakabandi, K., Sturdevant, D.E., Virtaneva, K., et al. (2014). Exposure-dependent control of malaria-induced inflammation in children. PLoS Pathog. *10*, e1004079.

Reed, L.J., and Muench, H. (1938). A simple method of estimating fifty percent endpoints. Am. J. Epidemiol. *27*, 493–497.

Rhein, B.A., Powers, L.S., Rogers, K., Anantpadma, M., Singh, B.K., Sakurai, Y., Bair, T., Miller-Hunt, C., Sinn, P., Davey, R.A., et al. (2015). Interferon-γ Inhibits Ebola Virus Infection. PLoS Pathog. *11*, e1005263.

Rhodes-Feuillette, A., Bellosguardo, M., Druilhe, P., Ballet, J.J., Chousterman, S., Canivet, M., and Périès, J. (1985). The interferon compartment of the immune response in human malaria: II. Presence of serum-interferon gamma following the acute attack. J. Interferon Res. *5*, 169–178.

Rogers, K.J., and Maury, W. (2018). The role of mononuclear phagocytes in Ebola virus infection. J. Leukoc. Biol. *104*, 717–727.

Rogers, K.J., Brunton, B., Mallinger, L., Bohan, D., Sevcik, K.M., Chen, J., Ruggio, N., and Maury, W. (2019). IL-4/IL-13 polarization of macrophages enhances Ebola virus glycoprotein-dependent infection. PLoS Negl. Trop. Dis. *13*, e0007819.

Rosenke, K., Adjemian, J., Munster, V.J., Marzi, A., Falzarano, D., Onyango, C.O., Ochieng, M., Juma, B., Fischer, R.J., Prescott, J.B., et al. (2016). *Plasmodium* Parasitemia Associated With Increased Survival in Ebola Virus-Infected Patients. Clin. Infect. Dis. *63*, 1026–1033.

Rosenke, K., Mercado-Hernandez, R., Cronin, J., Conteh, S., Duffy, P., Feldmann, H., and de Wit, E. (2018). The Effect of Plasmodium on the Outcome of Ebola Virus Infection in a Mouse Model. J. Infect. Dis. *218* (*suppl_5*), S434–S437.

Scheerlinck, J.P. (1999). Functional and structural comparison of cytokines in different species. Vet. Immunol. Immunopathol. *72*, 39–44.

Schmidt, N.W., Butler, N.S., Badovinac, V.P., and Harty, J.T. (2010). Extreme CD8 T cell requirements for anti-malarial liver-stage immunity following immunization with radiation attenuated sporozoites. PLoS Pathog. *6*, e1000998.

Scholzen, A., and Sauerwein, R.W. (2013). How malaria modulates memory: activation and dysregulation of B cells in Plasmodium infection. Trends Parasitol. *29*, 252–262.

Shtanko, O., Reyes, A.N., Jackson, W.T., and Davey, R.A. (2018). Autophagy-Associated Proteins Control Ebola Virus Internalization Into Host Cells. J. Infect. Dis. *218* (*suppl_5*), S346–S354.

Smit, M.A., Michelow, I.C., Glavis-Bloom, J., Wolfman, V., and Levine, A.C. (2017). Characteristics and Outcomes of Pediatric Patients With Ebola Virus Disease Admitted to Treatment Units in Liberia and Sierra Leone: A Retrospective Cohort Study. Clin. Infect. Dis. *64*, 243–249.

Steffen, I., Lu, K., Yamamoto, L.K., Hoff, N.A., Mulembakani, P., Wemakoy, E.O., Muyembe-Tamfum, J.J., Ndembi, N., Brennan, C.A., Hackett, J., Jr., et al. (2019). Serologic Prevalence of Ebola Virus in Equatorial Africa. Emerg. Infect. Dis. *25*, 911–918.

Stephens, R., Culleton, R.L., and Lamb, T.J. (2012). The contribution of *Plasmodium chabaudi* to our understanding of malaria. Trends Parasitol. *28*, 73–82.

Su, Z., and Stevenson, M.M. (2000). Central role of endogenous gamma interferon in protective immunity against blood-stage *Plasmodium chabaudi* AS infection. Infect. Immun. *68*, 4399–4406.

Takada, A., Robison, C., Goto, H., Sanchez, A., Murti, K.G., Whitt, M.A., and Kawaoka, Y. (1997). A system for functional analysis of Ebola virus glycoprotein. Proc. Natl. Acad. Sci. USA *94*, 14764–14769.

Teo, T.H., Lum, F.M., Ghaffar, K., Chan, Y.H., Amrun, S.N., Tan, J.J.L., Lee, C.Y.P., Chua, T.K., Carissimo, G., Lee, W.W.L., et al. (2018). *Plasmodium* co-infection protects against chikungunya virus-induced pathologies. Nat. Commun. *9*, 3905.

Vernet, M.A., Reynard, S., Fizet, A., Schaeffer, J., Pannetier, D., Guedj, J., Rives, M., Georges, N., Garcia-Bonnet, N., Sylla, A.I., et al. (2017). Clinical, virological, and biological parameters associated with outcomes of Ebola virus infection in Macenta, Guinea. JCI Insight *2*, e88864.

Villegas-Mendez, A., Greig, R., Shaw, T.N., de Souza, J.B., Gwyer Findlay, E., Stumhofer, J.S., Hafalla, J.C., Blount, D.G., Hunter, C.A., Riley, E.M., and

Couper, K.N. (2012). IFN-γ-producing CD4+ T cells promote experimental cerebral malaria by modulating CD8+ T cell accumulation within the brain. J. Immunol. *189*, 968–979.

Waxman, M., Aluisio, A.R., Rege, S., and Levine, A.C. (2017). Characteristics and survival of patients with Ebola virus infection, malaria, or both in Sierra Leone: a retrospective cohort study. Lancet Infect. Dis. *17*, 654–660.

Wec, A.Z., Nyakatura, E.K., Herbert, A.S., Howell, K.A., Holtsberg, F.W., Bakken, R.R., Mittler, E., Christin, J.R., Shulenin, S., Jangra, R.K., et al. (2016). A "Trojan horse" bispecific-antibody strategy for broad protection against ebolaviruses. Science *354*, 350–354.

Weyer, J., Grobbelaar, A., and Blumberg, L. (2015). Ebola virus disease: history, epidemiology and outbreaks. Curr. Infect. Dis. Rep. *17*, 480.

STAR★METHODS

KEY RESOURCES TABLE

REAGENT or RESOURCE	SOURCE	IDENTIFIER
Antibodies		
Anti-mouse NK1.1	BioXCell	Cat: BE0036
		RRID: AB_1107737
		Clone: PK136
Anti-mouse CD4	BioXCell	Cat: BE0119
		RRID: AB_10950382
		Clone: YTS 191
Anti-mouse CD8α	BioXCell	Cat: BE0061
		RRID: AB_1125541
		Clone: 2.43
Rat IgG2b	BioXCell	Cat: BE0252
		RRID: AB_2687733
		Clone: RG7/11.1
LEAF anti-mouse interferon gamma (discontinued)	Biolegend	Cat: 517903
		Clone: AN-18
Bacterial and Virus Strains		
rVSV/EBOV GP	Ebihara et al., 2007	N/A
EBOV: Mayinga variant	Texas Biomedical Research Institute	GenBank: NC_001608
Mouse-adapted EBOV: Mayinga variant	Texas Biomedical Research Institute	GenBank: AF_499101
Biological Samples		
Human monocyte derived macrophages	DeGowan Blood Center, Univ. Iowa	https://uihc.org/degowin-blood-center
Mouse (C57BL/6J) peritoneal macrophages	The Jackson Laboratory	Resident cells isolated from the peritoneal compartment
Mouse (C57BL/6J) *Ifnar*$^{-/-}$ peritoneal macrophages	The Jackson Laboratory	Resident cells isolated from the peritoneal compartment
Mouse (B6.129S7) *Ifngr1*^{tm1Agt}/J peritoneal macrophages	The Jackson Laboratory	Resident cells isolated from the peritoneal compartment
Mouse (C57BL/6J) *Ifnar/Ifngr*$^{-/-}$ peritoneal macrophages	Bred in house	Resident cells isolated from the peritoneal compartment
Chemicals, Peptides, and Recombinant Proteins		
Atovaquone	Sigma-Aldrich	Cat: A7986
Critical Commercial Assays		
ELISA MAX Deluxe Set Mouse Interferon Gamma	Biolegend	Cat: 430805
Detoxi-Gel Endotoxin Removing Gel	ThermoFisher Scientific	Cat: 20339
Soluble trimerized Zaire Ebola Glycoprotein	John Dye, USAMRIID	N/A
Experimental Models: Cell Lines		
Vero E6	ATCC	Cat: CRL-1586
Experimental Models: Organisms/Strains		
Mouse: BALB/cJ	The Jackson Laboratory	JAX: 000651
Mouse: B6.129S7-*Ifngr1*^{tm1Agt}/J	The Jackson Laboratory	JAX: 003288
Mouse: C57BL/6J	The Jackson Laboratory	JAX: 000664
	John Harty, Uiowa	
Mouse: C57BL/6J *Ifnar*$^{-/-}$	The Jackson Laboratory	JAX: 028288

(*Continued on next page*)

Continued		
REAGENT or RESOURCE	SOURCE	IDENTIFIER
Mouse: C57BL/6J *Ifnar/Ifngr*$^{-/-}$	Bred in house	N/A
Oligonucleotides		
See Table S1		N/A

LEAD CONTACT AND MATERIALS AVAILABILITY

No unique reagents were generated for this study. All materials and protocols are available upon request from the Lead Contact, Wendy Maury (wendy-maury@uiowa.edu).

EXPERIMENTAL MODEL AND SUBJECT DETAILS

Mice

Wild-type BALB/cJ mice were purchased from The Jackson Laboratory (stock #000651). C57BL/6 IFN-α/β receptor-deficient (*Ifnar*$^{-/-}$) were purchased from The Jackson Laboratory (stock #028288). Wild-type C57BL/6 mice were a kind gift from Dr. John Harty, University of Iowa. C57BL/6 *Ifnar*$^{-/-}$ *Ifngr1*$^{-/-}$ mice were generated by crossing C57BL/6 *Ifnar*$^{-/-}$ and C57BL/6 *Ifngr1*$^{-/-}$ mice (*Ifngr1*^{tm1Agt}/J Jackson Labs stock #003288). Genotyping was performed using primers and standard PCR conditions from Jackson labs. This study was conducted in strict accordance with the Animal Welfare Act and the recommendations in the Guide for the Care and Use of Laboratory Animals of the National Institutes of Health. The University of Iowa (UI) Institutional Assurance Number is #A3021-01. The Emory University Institutional Assurance Number is A3180-01. The Texas Biomedical Research Institute (TBRI) Institutional Assurance Number is A3082-01. All mouse procedures performed at the UI were approved by the UI Institutional Animal Care and Use Committee (IACUC) which oversees the administration of the IACUC protocols and the study was performed in accordance with the IACUC guidelines (Protocol #8011280). All mouse procedures performed at TBRI were approved by their Institutional Animal Care and Use Committee (IACUC) which oversees the administration of the IACUC protocols and the study was performed in accordance with the IACUC guidelines (Protocol #1645MU). All NHP procedures were performed at the Yerkes National Primate Research Center (YNPRC), an Association for Assessment and Accreditation of Laboratory Animal Care (AAALAC) international-certified institution. All NHP procedures were reviewed and approved by Emory University's IACUC (Protocol #Y2003225).

Nonhuman primate Plasmodium cynomolgi infections

NHP sera used in this study came from NHPs that were experimentally infected with *P. cynomolgi* at the Yerkes National Primate Research Center (YNPRC), an Association for Assessment and Accreditation of Laboratory Animal Care (AAALAC) international-certified institution. All procedures were reviewed and approved by Emory University's IACUC, and all NHPs were socially housed in pairs during infections. All housing was in accordance with Animal Welfare Act regulations as well as the Guide for the Care and Use of Laboratory Animals. A detailed description of the experimental design, infections, clinical data, etc., for the samples that were used in this manuscript were previously described in Joyner et al. (2016). Briefly, five malaria-naive, male, rhesus macaques (*Macaca mulatta*) of Indian origin were infected with 2,000 *P. cynomolgi* M/B strain sporozoites and parasitemia monitored daily by light microscopy up to 100 days post-inoculation. Plasma was isolated from blood collections prior to inoculation (i.e., Pre-Infection) and during acute, primary infections after performing a Lymphoprep PBMC isolation according to the manufacturer's suggested protocol. All samples were aliquoted and stored at −80°C until needed for experiments.

rVSV/EBOV GP stocks

Recombinant vesicular stomatitis virus encoding and expressing the glycoprotein from EBOV (Mayinga) was generated as previously described (Ebihara et al., 2007). Virus was propagated by infecting Vero cells at low MOI (~0.05) and collecting supernatants at 48hpi. The resulting supernatants were filtered through a 45 micron filter and purified by ultra-centrifugation (28,000 g, 4°C, 2 hr) through a 20% sucrose cushion. The resulting stocks were resuspended in a small volume of PBS and those used for *in vivo* studies were further purified by treatment with an endotoxin removal kit (Detoxi-Gel Endotoxin Removing Gel, ThermoFisher Scientific 20339) before being aliquoted and stored at −80°C until use. All viral titers were determined by $TCID_{50}$ assay on Vero cells.

WT EBOV stocks

All experiments with replication-competent EBOV were performed in the Animal Biosafely Level 4 (ABSL4) laboratory at the TBRI (San Antonio, TX). The wild-type EBOV and mouse-adapted EBOV (ma-EBOV), both variant Mayinga (NCBI accession numbers NC_001608 and AF_499101, respectively), were obtained from the virus repository at TBRI. EBOV stocks were generated and characterized as previously described (Bray et al., 1998; Shtanko et al., 2018).

Plasmodium infections and parasite quantification

Plasmodium yoelii (clone 17XNL, obtained from MR4, ATCC) and *Plasmodium chabaudi chabaudi* AS(Pyr1) (clone MRA-747, obtained from beiresources) infections were initiated by a serial transfer of 10^6 parasitized red blood cells (pRBCs) i.v. Control RBCs were isolated from naive C57BL/6 mice aged 6-8 weeks, 10^6 RBCs were transferred. To inactive iRBCs, 5mL of iRBCs were irradiated with 200 Gy by cesium irradiation. Parasitemia was measured using flow cytometry as previously described (Malleret et al., 2011). Briefly, 1 μL of blood was obtained by milking the tail vain and mixed to 100uL of PBS. The cells were spun down and resuspended in 100 μL of staining cocktail containing Hoechst-34580 (1:1000, Thermo Fisher Scientific), Dihydroethidium (1:500, Thermo Fisher Scientific), CD45.2-FITC (1:200, clone:104, Biolegend) and TER-119-APC (1:400, clone: TER-119, Tonbo) and incubated for 30 minutes at 4°C. The cells were washed with PBS and spun down at 200 x g for 5 minutes and run on FACSVerse after resuspending in 100μL of PBS. Percentage RBCs staining positive for Hoechst 34580 and Dihydroethidium indicative of parasitized cells were calculated using FlowJo software (Treestar Inc.).

METHOD DETAILS

BSL-4 mouse experiments

Study #1 consisted of 6 groups of 10 five-week-old female BALB/c mice. On day −6 relative to ma-EBOV exposure, 3 groups of mice were injected with 10^6 *Plasmodium yoelii*-infected RBCs as described above. Subsequently, parasite-exposed and naive animals were transferred to the ABSL4 for acclimation. On day −1, blood was collected from a submandibular vein of a subset of mice in each group to confirm parasitemia. On day 0, groups were challenged with either 1, 10, or 100 plaque-forming units (PFU) of ma-EBOV (as accessed on Vero cells) via the intraperitoneal route. Animals were observed at least twice daily for morbidity and mortality for 18 days after virus challenge. Group clinical scores were recorded as the sum of all clinical observations for the group. If a clinical score of ≥ 12 was reached, the animal was considered "terminally ill" and euthanized. On day 3, three animals from each group were euthanized, and blood, liver and spleen were collected to determine viremia and virus loads. The viral titers in the blood was determined after serum isolation, using the neutral red plaque assay, and virus load in tissues by qRT-PCR as described below. The remaining 7 mice in each group served to determine animal survival.

Study #2 consisted for 4 groups of 10 five-week-old female BALB/c mice. Protocols were identical to those described above, except only the two lower doses of ma-EBOV were used. Data from the two different 1 and 10 iu challenge studies were pooled for analysis.

BSL-2 mouse experiments

For *in vivo* infections with rVSV/EBOV GP, the lowest dose of virus providing consistent lethality was determined in *C57BL/6 Ifnar*$^{-/-}$ mice. This was found to be 10^2 iu for males and $5x10^2$ iu for females. Virus was administered in 100 μL sterile PBS by intraperitoneal injection. For atovaquone treatments, drug was administered at 25 mg/kg by ip injection on days 6-8. For experiments with IFN-γ, drug was administered at the indicated dose and time suspended in 100 μL sterile PBS. For depletion studies, mice were given 200 μg of the indicated antibodies 24 hours after administration of *Py.*

Antibodies: anti-mouse NK1.1 BioXCell clone PK136, anti-mouse CD4 BioXCell clone YTS 191, anti-mouse CD8 alpha BioXCell clone 2.43, IgG controls Rat IgG2b BioXCell clone RG7/11.1.

Titer assay (BSL-2)

To obtain titers, serum samples were filtered through 45 μm filters and serially diluted before being added onto Vero cells. Titers were calculated as 50% tissue culture infectious dose per milliliter of serum ($TCID_{50}$/mL) according to the Reed-Muench method (Reed and Muench, 1938).

Organ Harvest

Mice were anesthetized using isoflurane and perfused through the left ventricle with 10 mL cold sterile PBS prior to being euthanized by rapid cervical dislocation in accordance to our IACUC protocol. Organs were harvested and snap frozen in liquid nitrogen to preserve virus. Organs were homogenized in 1mL TRizol regent using the "gentleMACS Dissociator" with M tubes (Miltenyi Biotec).

qRT-PCR

RNA was isolated using the TRIzol reagent from Invitrogen. All steps were performed according to the manufacturer's specifications. RNA was subsequently converted to cDNA with the High Capacity cDNA RevTrans Kit (#4368814) from Applied Biosystems. A total of 1 μg of RNA was used as input for each reaction. Quantitative PCR was performed using POWER SYBR Green Master Mix (#4367659) from Applied Biosystems according to the manufacturer's instructions and utilizing a 7300 real time PCR machine from Applied Biosystems. 20ng of cDNA were used in each well. Primers are available in Table S1.

ELISAs

Interferon gamma was detected using the "Mouse IFN-γ ELISA MAX" kit from Biolegend (#430805) in accordance with manufacturer's instructions. Detection of anti-EBOV GP antibodies was performed by coating optical plates overnightwith soluble EBOV

GP (50 μl/well at 10 μg/ml). Wells were washed 2x with PBST (0.015% Tween 20), blocked for 1 hour (PBS 2%BSA), washed 3x with PBST, and incubated overnight in 4°C with either a standard curve composed of fractionated mouse immunoglobulin (Immunoreagents #Mu-003-B) or serum samples. Following incubation wells were washed 4x with PBST and incubated with 50 μL rabbit anti-mouse IgG heavy and light chain-HRP (10 μg/ml Pierce #31457) for 1 hr at RT. Wells were then washed 5x with PBST, incubated with 50 μL of HRP substrate (BD OptEIA #555214). The reaction was stopped with 50 μL 2M H_2SO_4 and absorbance at 450nm was measured on Synergy H1 hybrid reader. Total concentration of anti-EBOV GP antibodies was quantified by comparison to the standard curve.

Serum isolation and *ex vivo* treatments

Whole blood was obtained by facial vein puncture in accordance with IACUC guidelines (https://animal.research.uiowa.edu/iacuc-guidelines-blood-collection). Serum was isolated by centrifugation (90 s, 8000 x g) in serum separator tubes (BD Microtainer #365967). Serum was passed through 45 μm filters prior to use. For *ex vivo* experiments, serum was either added directly to macrophages or pretreated for 15 minutes with 1 μL LEAF anti-mouse IFN-γ antibody (1mg/ml) (Clone AN-18, Biolegend #517903). Serum with or without antibody was left on macrophages for 24 hours and removed at the time of infection.

Macrophage isolations

Peritoneal cells were obtained from mice by peritoneal lavage with 10mL of RPMI + 1% pen/strep. For studies utilizing resident peritoneal macrophages, cells were washed once with PBS and resuspended in RPMI containing 10%FBS, 1% pen/strep, 1% non-essential amino acids (NEAA), and 1% sodium pyruvate. After 48 hours, cells were washed with PBS which removed most of the non-adherent cells. This generated a macrophage enriched population of cells.

Human macrophages were matured from monocytes obtained from leukocyte reduction cones containing peripheral blood from healthy donors at the DeGowin Blood Center at University of Iowa Hospitals and Clinics. Peripheral blood mononuclear cells were purified by Ficoll gradient, and monocytes were enriched by adherence to tissue culture flasks coated in 2% gelatin and pre-treated with human plasma. Following isolation, monocytes were plated in RPMI with 10%FBS, 1% pen/strep, 1% non-essential amino acids (NEAA), 1% sodium pyruvate, and 20ng/mL human MCSF. Cells were allowed to mature for 6 days at which point they were washed with PBS to remove non-adherent cells.

QUANTIFICATION AND STATISTICAL ANALYSIS

In vivo experiments: significance was defined as $p < 0.05$ given alpha = 0.05 using Log-rank (Mantel-Cox) test. N is indicated on the figure legends. *Ex vivo* experiments: significance was determined by two tailed unpaired Student's t test (alpha = 0.05). For panels where multiple comparison were made, a line is shown to indicate the comparison made. Individual data points are shown. All statistics were calculated using GraphPad Prism 8 software (GraphPad Software, Inc.).

DATA AND CODE AVAILABILITY

All data are available from the Lead Contact upon reasonable request.

Cell Reports, Volume *30*

Supplemental Information

Acute *Plasmodium* Infection Promotes Interferon-Gamma-Dependent Resistance to Ebola Virus Infection

Kai J. Rogers, Olena Shtanko, Rahul Vijay, Laura N. Mallinger, Chester J. Joyner, Mary R. Galinski, Noah S. Butler, and Wendy Maury

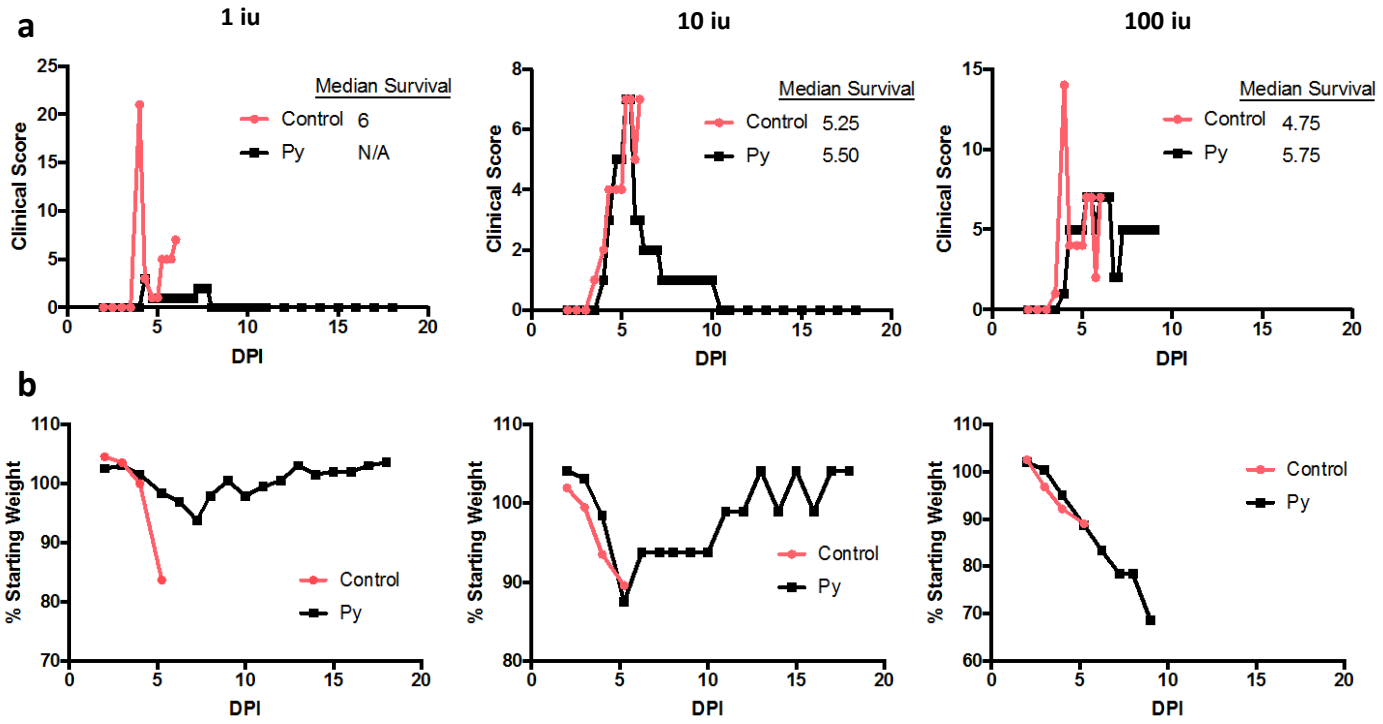

Figure S1: Acute *Plasmodium* infection in mice protects against EBOV challenge, Related to Figure 1. WT BALB/c mice were infected with $1x10^6$ *Plasmodium yoelli* iRBCs and challenged with 1, 10 or 100 iu ma-EBOV (Mayinga) 6 days later. Mice were monitored up to 4 times daily during the critical phase and morbidity was assessed. Shown are clinical scores **(a)** and weight loss **(b)**. Data are expressed as either aggregate clinical scores or average weights compiled from all surviving mice at the time of observation (n=1-7). Statistical analyses were not performed as each point represents an average value of a variable number of mice depending on the number of surviving animals.

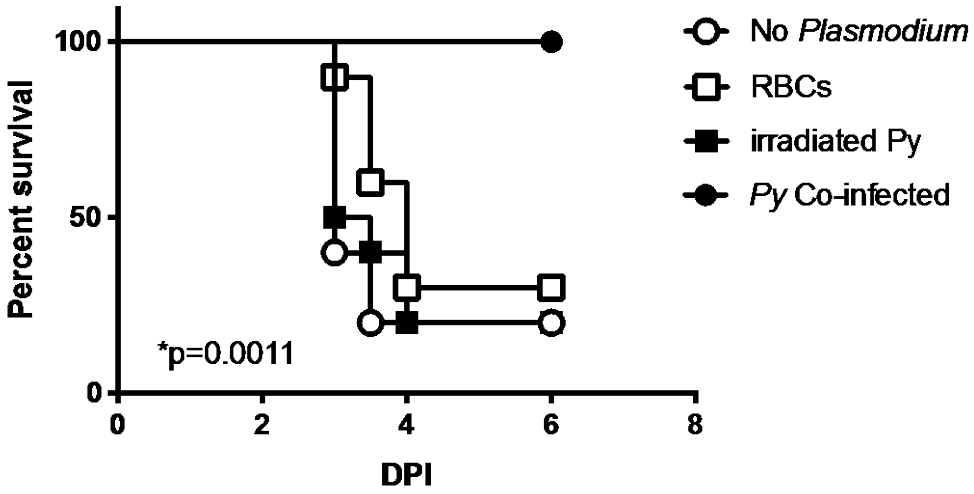

Figure S2: RBCs and irradiated *Py* iRBCs do not protect from rVSV/EBOV GP challenge, Related to Figure 2. C57BL/6 *Ifnar*$^{-/-}$ mice were inoculated i.v. with 10^6 of the indicated RBCs (*Py* infected, uninfected, or irradiated). Mice were challenged with a lethal dose of rVSV/EBOV GP 6 days later. Survival was monitored. n=10 per group.

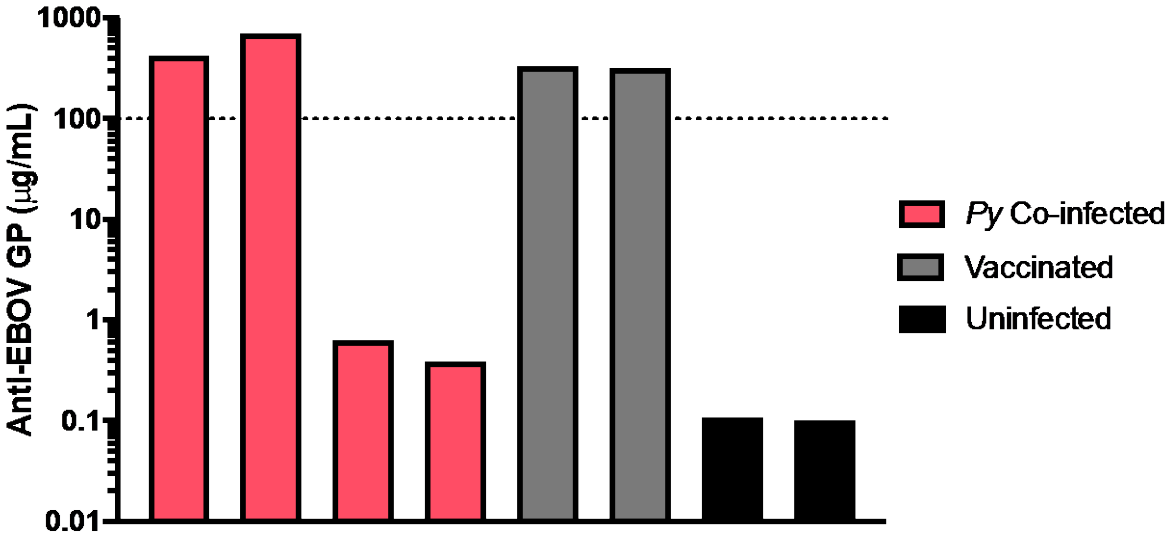

Figure S3: EBOV GP antibody production in *Py* infected mice, Related to Figure 2. C57BL/6 *Ifnar*$^{-/-}$ mice were infected i.v. with 1x10^{6} *Plasmodium yoelli* iRBCs. These mice were challenged with a dose of rVSV/EBOV GP that is lethal to naïve mice (red) or 1e3 EBOV pseudovirions (gray) 6 days later. Anti-GP antibodies in the serum at day 21 were measured by ELISA. Line represents the amount of antibody previously found to be predictive of protection against ma-EBOV challenge. Each bar represents an average of 2 replicates from a single mouse.

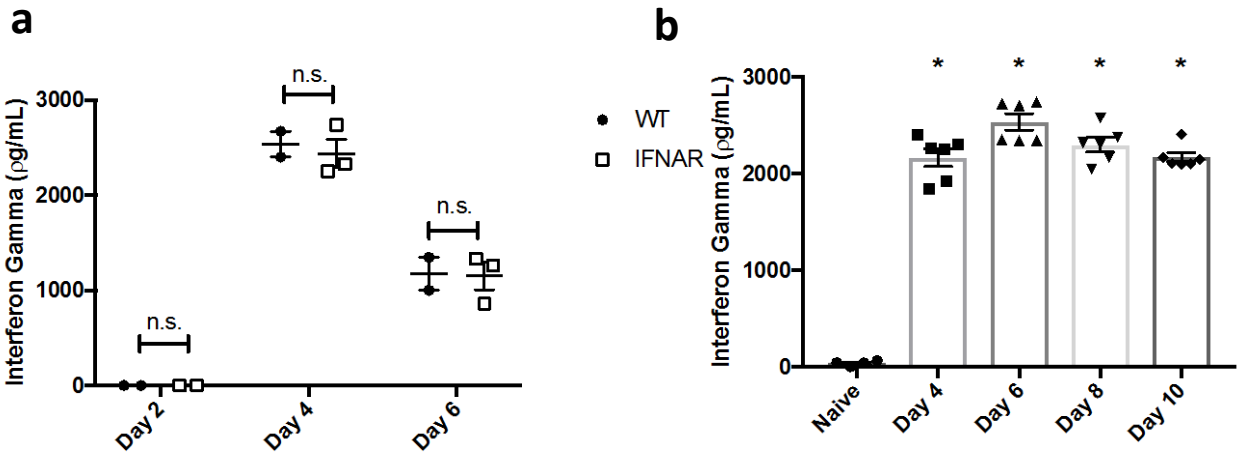

Figure S4: *Plasmodium yoelii* infection robustly stimulates serum IFN-γ levels in WT, *Ifnar*$^{-/-}$ and *Ifnar/Ifngr*$^{-/-}$ mouse strains, Related to Figure 3. a) WT BALB/c (closed squares) or BALB/c *Ifnar*$^{-/-}$ (open squares) mice were infected with 1x10^{6} *Plasmodium yoelli* iRBCs and IFN-γ production was measured by ELISA at the indicated times after infection. **b)** C57BL/6 *Ifnar/Ifngr*$^{-/-}$ mice were infected with 1x10^{6} *Plasmodium yoelli* iRBCs. At the indicated times after infection, serum was harvested and IFN-γ was measured by ELISA. For all experiments, * indicates $p<0.05$.

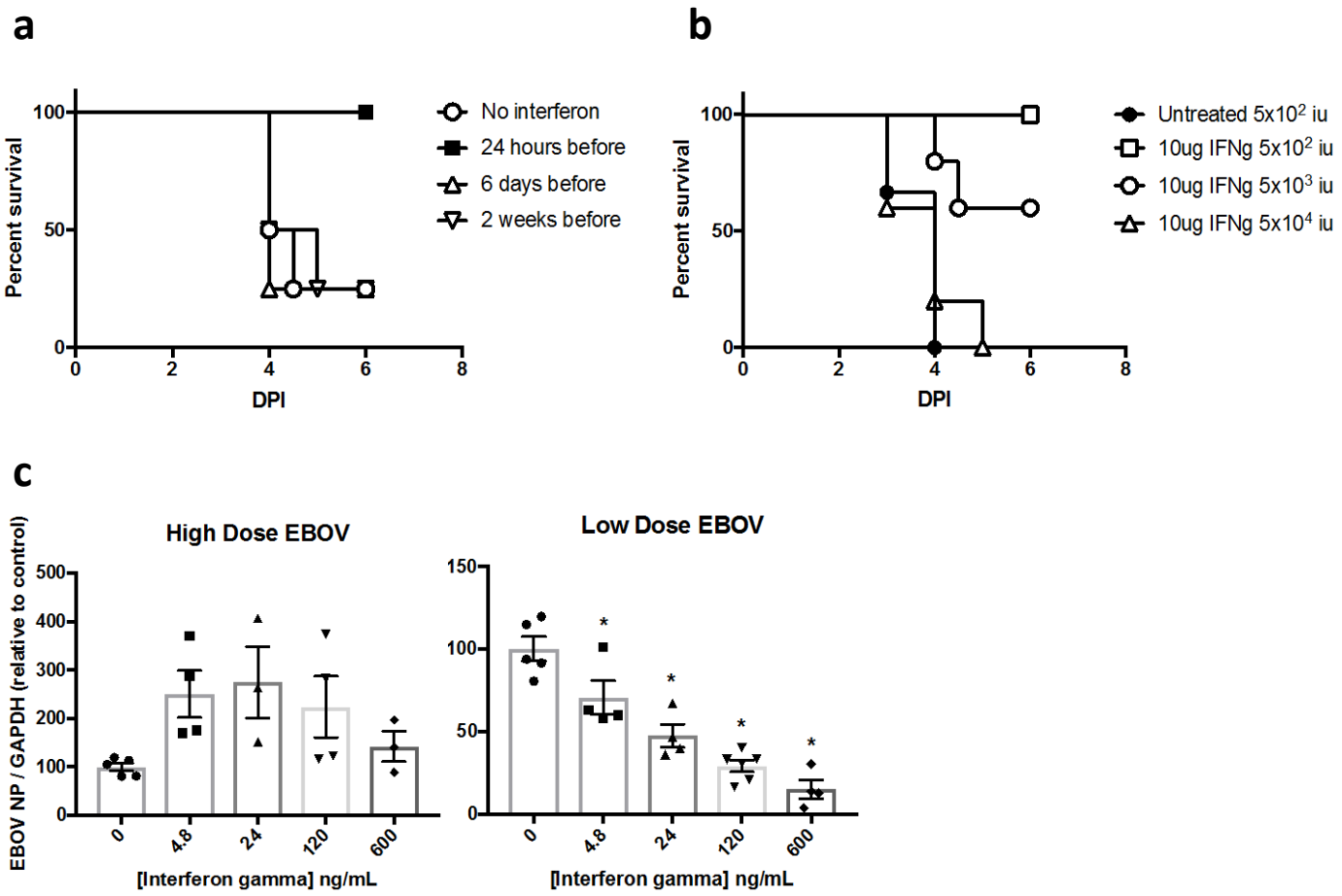

Figure S5: Amount and timing of rVSV/EBOV GP delivered is critical for IFN-γ mediated protection from infection, Related to Figure 5. a) *Ifnar*$^{-/-}$ mice were injected with 5µg IFN-γ at the indicated times prior to challenge with rVSV/EBOV GP. Mice were observed daily (n=4/group). **b)** *Ifnar*$^{-/-}$ mice were injected with 5µg IFN-γ 24 hours prior to challenge with the indicated amount of rVSV/EBOV GP (n=3 untreated, n=5 for each treated group). Mice were observed daily. **c)** *Ifnar*$^{-/-}$ pmacs were treated with varying concentrations of IFN-γ and infected with ma-EBOV under BSL-4 conditions 24 hours later. Cells were infected with either a high dose (2000 pfu) or low dose (200 pfu) of EBOV. RNA was isolated 24 hpi and virus replication was quantified by qRT-PCR for EBOV NP gene expression.